AIP Applied Physics Letters

Heterodyne interference lithography for one-step micro/nano multiscale structuring

Bongchul Kang, Jiwhan Noh, Joohyung Lee, and Minyang Yang

Citation: Applied Physics Letters **103**, 243110 (2013); doi: 10.1063/1.4841435
View online: http://dx.doi.org/10.1063/1.4841435
View Table of Contents: http://scitation.aip.org/content/aip/journal/apl/103/24?ver=pdfcov
Published by the AIP Publishing

Heterodyne interference lithography for one-step micro/nano multiscale structuring

Bongchul Kang,[1,2,a),b)] Jiwhan Noh,[3,a)] Joohyung Lee,[4] and Minyang Yang[5,c)]
[1]*Department of Mechatronics Engineering, Gyeongnam National University of Science and Technology, Jinju 660-758, South Korea*
[2]*School of Engineering and Applied Sciences, Harvard University, 9 Oxford Street, Cambridge, Massachusetts 02138, USA*
[3]*Division of Laser Applied Machine Development, Korea Institute of Machinery and Materials, Daejeon 305-343, South Korea*
[4]*Center for Space Optics, Korea Research Institute of Standards and Science, Daejeon 305-340, South Korea*
[5]*Department of Mechanical Engineering, Korea Advanced Institute of Science and Technology, Daejeon 305-701, South Korea*

(Received 25 April 2013; accepted 18 November 2013; published online 12 December 2013)

A heterodyne interference lithography method using two slightly different wavelengths for one-step multi-scale fabrication of micro/nano hybrid structures is presented. This method has been used to locally fabricate one- and two-dimensional periodical sub-wavelength nanopatterns with a spatial periodicity of several micrometers. Furthermore, multilayered nanostructures with different layer compositions were fabricated by simply controlling the intensity ratio of the two wavelengths. As a result, this method can cost-effectively maximize the degree of freedom of the interference lithography method. The heterodyne interference lithography method can potentially be used in the fabrication of unconventional bio-mimetically engineered surfaces as well as heterocomplexed optics. © *2013 AIP Publishing LLC*. [http://dx.doi.org/10.1063/1.4841435]

Photolithography can fabricate structures larger than the operating wavelength. Unfortunately, conventional photolithography is limited to fabricate nanoscale features much smaller than the wavelength owing to the theoretical limit of light diffraction.[1] To improve the resolution, photolithography is inevitably moving towards ultra-short wavelengths such as extreme ultra-violet (UV) or X-ray. However, these systems are complex and expensive, and they require specialized components compatible with high photon energies. In addition, these methods require an expensive mask fabricated by expensive e-beam lithography for each pattern design.[2] If it could also make features arbitrary smaller than the wavelength, we can easily make a wide variety of nanodevices without above great efforts. Interference lithography (IL) is a low-cost and mask-free nanofabrication method for making periodical line or dot-shaped nanopatterns less than the wavelength in parallel.[3–6] IL is a conceptually simple process where two coherent beams interfere to produce a standing wave, which is recorded in a photoresist (PR). Theoretically, the smallest attainable period is $\lambda/(2\sin\theta\cdot n)$, where λ is the laser wavelength, θ is the half-angle between the interfering beams, and n is the refractive index of the medium.[6] Previously, most IL studies focused on improving the resolution in order to overcome the theoretical relationship, which included techniques such as atomic beam interference, achromatic interferometric lithography (AIL), and spatial frequency multiplication process.[7–9] Most applications of IL are limited to simple optics, such as linear scales, wire grid polarizers, and other diffractive optics, because IL is capable of making only fixed periodic nanopatterns over the entire substrate.[10–12] If, however, nanostructures and microstructures can exist while spatially sharing a domain using a single fabrication method, it is expected that the combined effect of the microstructure and nanostructure will be cost-effectively implemented in unconventional nanodevices such as heterogeneous biomimetic nanosurface, bundled photonic crystals, and integrated micro/nano-optics. Unfortunately, it is a great challenge to realize a hybrid structure including both micro- and nanofeatures using aforementioned fabrication techniques because multiple fabrication steps with specially designed tools are needed to integrate these two completely different scale regimes, making it prohibitively expensive. Therefore, efficiently exploring the combined effect of nano and microscale regimes requires a multiscale fabrication method that is both simple and inexpensive.

In this paper, we report the heterodyne interference lithography (HIL) method to form nanopatterns with a resolution less than the laser wavelength periodically placed at a distance of several micrometers as a one-step multiscale fabrication process.

The two-different interference fringes were independently generated by individual interference of two different coherent lights, as shown in Fig. 1(a). If these lights originated from a single laser cavity and the independently generated interference fringes spatially overlapped in a single domain, then the interference fringes could interfere again with each other because of the coherency of the pre-interfered fringes. By assuming that the wavelengths are very close to each other in the spectral domain ($\Delta\lambda \ll \lambda$),[13,14] the intensity of the heterodyne interference fringe (HIF) can appear as a spatial-beating phenomenon with a much longer period than that of the wavelength, unlike the conventional sinusoidal appearance of pre-interfered fringes. To theoretically verify this phenomenon in IL, the HIF pattern was

[a)]B. Kang and J. Noh contributed equally to this work.
[b)]Electronic mail: kbc6039@gntech.ac.kr
[c)]Electronic mail: myyang@kaist.ac.kr

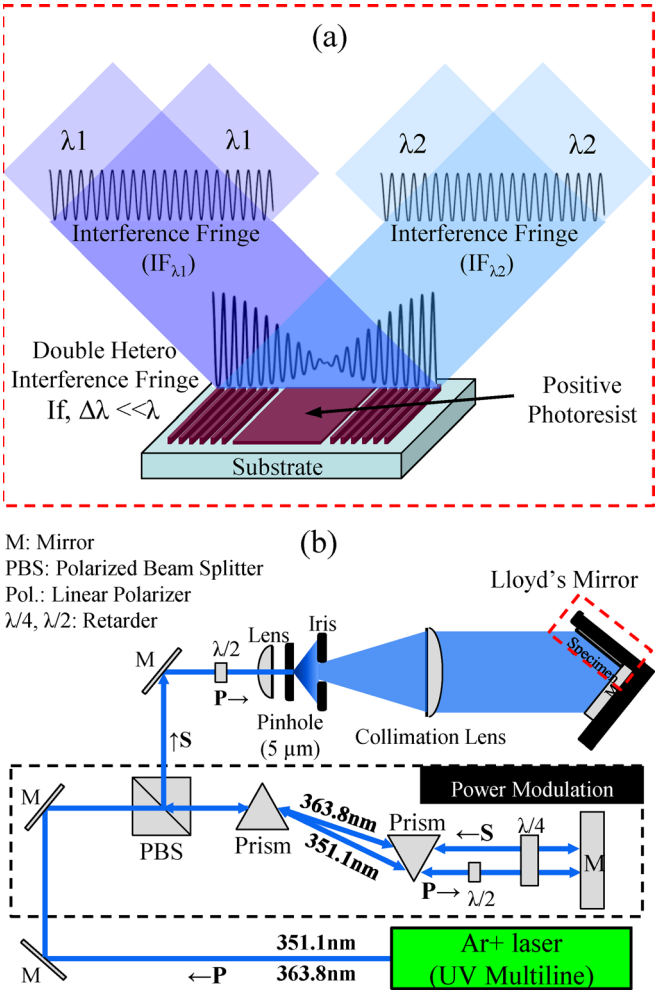

FIG. 1. (a) Conceptual illustration of heterodyne interference lithography. (b) Experimental setup for heterodyne interference lithography (black square box: intensity modulation depending on wavelengths, red square box: Lloyd's mirror).

derived using the theoretical interference relationship of coherent light,[15] when the intensities of the two beam are identically and the incident angle is 45°, according to the following equation:

$$I_{hetero} = 4I\left[1+\cos\left(\frac{\sqrt{2}\pi(\lambda_1+\lambda_2)d}{\lambda_1\lambda_2}\right)\times\cos\left(\frac{\sqrt{2}\pi d\cdot\Delta\lambda}{\lambda_1\lambda_2}\right)\right]^2, \quad (1)$$

where I_{hetero} is the intensity of HIF, I is the intensity of laser beam, d is the spatial distance, λ_1 and λ_2 are the wavelengths of two beams, and $\Delta\lambda$ is the wavelength difference of two beams. The interference equation is expressed by the multiplexing of a rapidly oscillating term by single-wavelength interference and a slowly oscillating term of the beating of two wavelengths, as shown in Eq. (1). Therefore, the HIF simultaneously contains both the long periodical beating component of several microns and the periodical component of original interference, which can be modulated constructively and destructively with a period of several micrometers, as shown in Fig. 1(a).

By applying the heterodyne interfered light to a positive PR, the nanopatterns did not form only in the destructive interference region due to the lack of dose required for the PR development; otherwise, the PR layer exposed in the constructive region was locally developed with an original interference nanoperiod, as shown in Fig. 1(a). Therefore, the PR nanopatterns generated by the original spatial frequency collectively occurred and disappeared with a spatial period of several micrometers. Heterodyne interference lithography is an interesting attempt elevating temporal heterodyne technology used in signal processing into spatial nanofabrication technology.[13,14]

Conventional argon ion (Ar+) lasers typically emit at 13 different wavelengths from UV to the near-infrared region of spectrum.[16] However, it has been characterized that most of the emitted energy of multiline UV Ar+ laser is concentrated on two wavelengths, 351.1 nm (~44%) and 363.8 nm (~36%).[16] We employed a multiline continuous wave UV Ar+ laser (INNOVA 300 Coherent Co.) as the spectrum is compatible with conventional PRs, and the wavelength difference of 12.7 nm is sufficiently narrow. The well-known Lloyd's mirror system consisting of a mirror fixed perpendicular to the specimen was employed to generate interference fringes, as highlighted within the red box of Fig. 1(b).[6] An additional setup located in front of the Lloyd's mirror was needed to adjust the intensity ratio of the two different wavelengths due to the non-negligible intensity discrepancy depending on the wavelength of the laser, as highlighted within the black box of Fig. 1(b). A prism pair was used to split the original laser spatially into two beams by the wavelength, allowing for independent polarization adjustments. Both beams passed through a $\lambda/4$ plate twice, to be reflected by a polarizing beam splitter. Here, the intensity of the 351.1 nm beam was adjusted to match that of 363.8 nm beam by rotating an additional $\lambda/2$ plate. The beams were recombined into a single beam by the prism pair and retroreflected by the polarizing beam splitter. The polarization of the recombined beam, which had changed to S-polarization, was transferred back to P-polarization by using another $\lambda/2$ plate in front of a spatial filter in order to enhance the selectivity of the interference fringes.[17] Finally, the recombined laser beam was spatially filtered using a lens of focal length 30 mm followed by a 5 μm pinhole, and then collimated with a lens of focal length 300 mm. This resulted in a 100 mm diameter beam with a uniform intensity distribution at the entrance to the Lloyd's system.

A silicon wafer used as a substrate was cleaned using acetone in an ultrasonic bath followed by hexamethyldisilazane solution spun at 3000 rpm. Following this, AZ1500 positive PR was spun on the wafer while adjusting the rotation speed. Here, the film thickness gradually decreased from 800 nm to 250 nm, with an increase in the speed from 1500 rpm to 3000 rpm. The wafer was then soft baked at 90 °C for 30 s. The prepared specimen was exposed using the designed HIL system at a fixed total laser intensity of 5 mW/cm^2 (351.5 nm at 2.5 mW/cm^2 and 363.8 nm at 2.5 mW/cm^2). The dose was varied between 150 and 450 mJ/cm^2 by adjusting the exposure time as required for the particular nanostructure size and PR thickness. The baked specimen was immersed for PR development in the diluted developing solution (1:4 ratio of AZ 400 K:distilled water).

The formula derived in Eq. (1) was numerically calculated using Matlab software to graphically confirm the expected 3D

intensity profile. In this calculation, the undefined terms in the formula were substituted by $\lambda_1 = 351.1$ nm, $\lambda_2 = 363.8$ nm, $\Delta\lambda = 12.7$ nm, $d = 0 \sim 15000$ nm, and Δd (iteration step) $= 10$ nm. Fig. 2(a) shows the simulated 3D intensity profile of the HIF along the X-axis. The laser interference nanofringes have a period of the wavelength divided by the square root of 2, with the intensity of the nanofringe modulating sinusoidally as a group. The group period of the modulated nanofringe, which was determined by the wavelength difference, to be 7.1 μm. If $\Delta\lambda$ is larger than 12.7 nm, the group period would become smaller, according to the Eq. (1). The choice of two wavelengths used in this method should be limited in the narrow UV spectral band with wavelengths of tens of nanometers. If an excessively large wavelength difference from UV to visible range was used, the effect of visible light could disappear, because most PRs not only react with UV light but also beating phenomenon does not occur due to the large wavelength difference. Experimental studies were conducted to verify this numerical hypothesis. Fig. 2(b) shows the scanning electron microscope (SEM) image of a line-shaped PR structure fabricated using an exposure of 150 mJ/cm^2 and a 30 s development time. The line-shaped PR nanopatterns have a width of 100 nm and a period of 250 nm, as shown in the inset of Fig. 2(b). The nanopattern groups appeared and disappeared spatially with a period of 7.1 μm, which is in good agreement with the simulation result. It was observed that the boundary between the nanopatterned and pattern-free regions is more abrupt than the simulation result. Since most kinds of PR have their own specific energy thresholds required for development, only the PR exposed by that threshold could be developed discretely, in spite of the continuously varying intensity of the HIF.

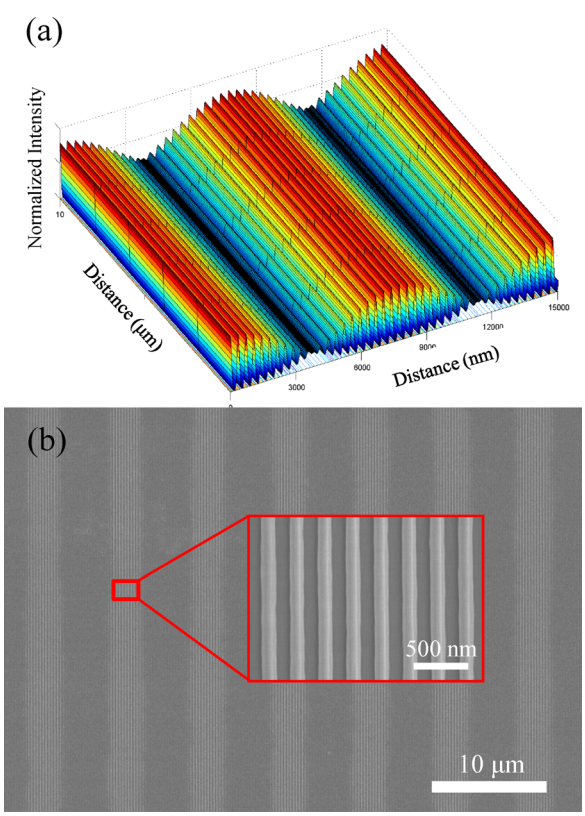

FIG. 2. (a) Numerical simulation result of the one dimensional heterodyne interference fringe. (b) SEM image of corresponding experimental result.

IL can also be used to fabricate two-dimensional (2D) PR nanopatterns using the multiple exposure technique that re-exposes the pre-exposed specimen after rotating the beam incident direction by 90°.[6] Here, as the PR in the un-exposed region is exposed, the pattern in the constructive region changes from continuous lines to islandlike dots. Fig. 3(a) shows PR structures fabricated by this exposure technique. At a glance, it can be easily associated with the usual checkerboard patterns. As the dots with 110 nm diameters were regularly arranged at periodic intervals of 250 nm in the patterned region and these patterned regions had a micro-period of 7.1 μm, as shown in Figs. 3(b)–3(d), the basic structure component is identical to that of the 1D patterning result shown in Fig. 2. The nanodots in the center of constructive interference region were well formed with a circular shape, because the developed area of conventional positive PRs was expanded by increasing the dose.[6] Otherwise, the boundary PR was partially connected to each other between the pattern groups due to the insufficient dose. To reflect the perpendicular rotation of the beam-incident direction for 2D structuring in the calculation, the 3D intensity profile of the 2D HIF was calculated by superimposing 1D intensity profiles along the X and Y-axes, respectively, as seen in Fig. 3(c). The region marked in red in Fig. 3(c) corresponds exactly to the center of Fig. 3(b).

Unlike the experiments conducted previously where the optical intensity between the two main wavelengths was maintained equivalently, to investigate the effect of wavelength-dependent intensity difference on pattern formation, the original laser with a total laser power of 5 mW/cm^2 was used without the intensity compensation. The nanopattern fabricated without the intensity compensation was composed of three major structural components: a large nanopattern group, a pattern-free group, and a small nanopattern group, as shown in Fig. 4(a). In particular, the small nanopattern groups were only observed in the central square of the four well-defined large nanopattern groups. As seen in the 2D heterodyne interference pattern shown in Fig. 3(d), the small nanopattern groups located in the central diagonal between the maximum exposure regions shows a destructive

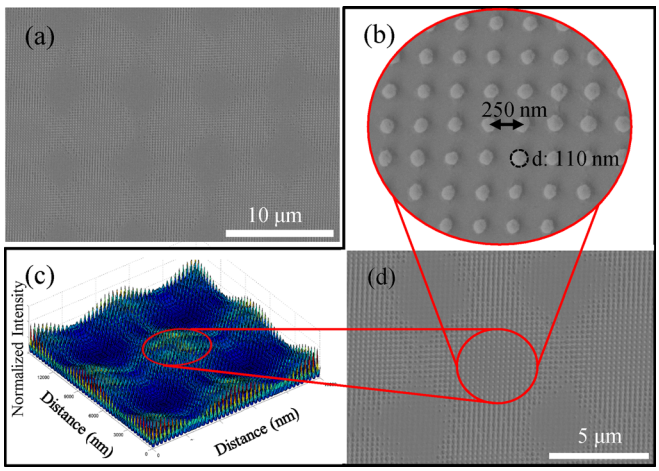

FIG. 3. (a) SEM image of photoresist in 2D heterodyne interference lithography, (b) locally magnified SEM images of PR, (c) the numerical simulation result of 2D heterodyne interference fringe, and (d) corresponding magnified SEM image of 2D HIL.

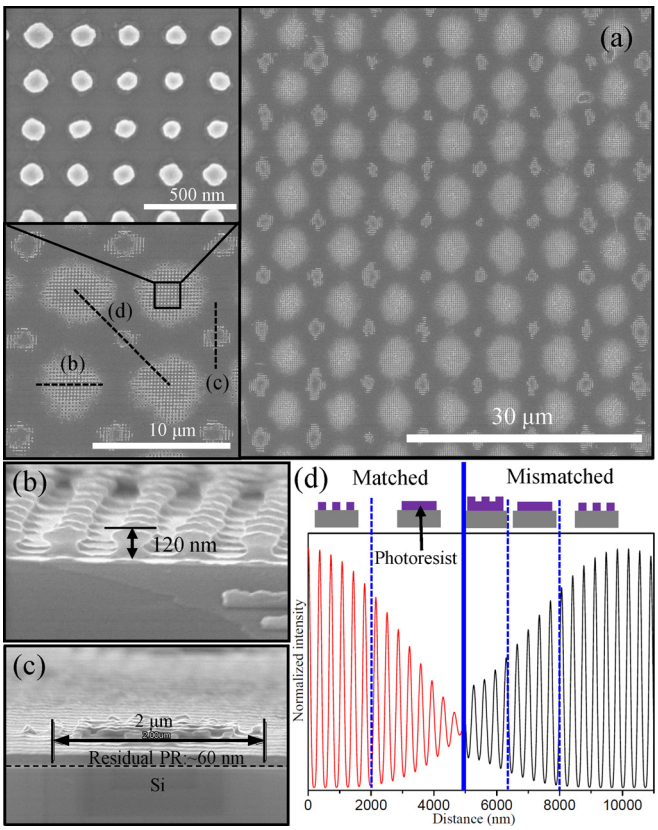

FIG. 4. (a) SEM images of PR in the un-matched intensity condition. Cross sectional SEM images of PR (b) in the constructive interference region and (c) in the destructive interference region. (d) Comparison of calculated intensity profiles along the dotted line (d) shown in Fig. 4(a) in the condition of intensity-unmatched (black line) and matched beams (red line). Inset is the schematic of developing behavior of PR according to the intensity modulation of two beams.

heterodyne interference region, as seen in the experiment and simulation results of Fig. 3. This is generated by spatially overlapping the destructive region of the 1D heterodyne interference fringes along the X and Y-axes, respectively.

The reason for the presence of the small nanopattern group can be found in the cross-sectional SEM images of the developed patterns, as shown in Figs. 4(b) and 4(c). As the height of the patterns in the large nanopattern group was 120 nm without a residual layer, it can be inferred that the patterns were fully developed even if the original coated PR thickness was 250 nm. Otherwise, the small nanopattern group with a lateral size of approximately 1.5–2 μm was created on the residual PR layer of a thickness of 60 nm. Since the intensity of the 351.1 nm beam was approximately 1.2 times higher than that of 363.8 nm beam in the original laser, the intensity level of the destructive HIF only increased locally compared to the mutually intensity-matched condition owing to the effect of the intensity difference, as shown in the simulation result of Fig. 4(d). The constructive HIF in Fig. 4(d) did not depend on the relative intensity difference between the two beams because the total intensity combing the two beams was fixed as a 5 mW/cm^2, and the HIF was created by the superposition of individual interference fringes. Therefore, the four large nanopattern groups formed by the constructive HIF were still created with a diagonal period of 10.0 μm around the small nanopattern group formed by the locally increased HIF level in the intensity-mismatched condition, as shown in Fig. 4(a). This period matched well with the simulation result of Fig. 4(d). In Fig. 4(d), the dose threshold corresponding to the highest intensity level in the destructive interference region of the intensity-mismatched condition overlaps spatially with the low-level nanofringes of 2.0 μm in the intensity-matched condition. The local intensity increase of the destructive HIF in the intensity-mismatched condition contributes to the creation of these unconventional double-layered small nanopattern groups among the large ones. Otherwise, only a thin 60 nm residual layer of PR was formed in the boundary between the large and small nanopattern groups, without any other pattern formations. As shown in the schematic inset of Fig. 4(d), this stepwise development of PR can be explained as follow. In the destructive region, the PR is developed slightly by the locally increased intensity on the residual PR. In the interstate region between the constructive and destructive HIF, the small PR patterns, which were slightly developed on the residual PR, are even removed by the enlargement of the developed area by overexposure and then a thin PR layer is only left on the wafer.[6,18,19] In constructive region, the residual layer is selectively developed with the periodicity of the original HIF as a result of the nearly identical intensity level of both cases in the constructive region. Therefore, it is reasonable to estimate that the local intensity enhancement only in the destructive HIF induces the stepwise developing behavior of the PR in the intensity-mismatched condition. These unique findings have not been reported previously either using IL techniques or other photolithography methods. Finally, it is expected that 2D and 3D PR nanostructures with more complicated and diverse shapes can be fabricated through relative laser power modulation.

The HIL method can potentially be applied to the emerging fields of biological as well as optical devices by expanding the application field of conventional ILs. Until recently, bio-mimetic surface studies have focused on fabricating superhydrophobic nanostructures, such as the leaf of a lotus plant, owing to its outstanding characteristics of low friction contact and high-resolution dewetting.[20] Unlike this lotus effect, the Cassie impregnating wetting state can incorporate a high contact angle with strong adhesive property between water and a solid surface.[21] This state can be found in the microscopy images of petal surface, such as that of red rose, where many nanostructures on the top of each micropapillae are periodically arrayed with a spacing of several micrometers on this surface. These hierarchical and hybrid micro- and nanostructures provide sufficient roughness for superhydrophobicity but have a high adhesive force with water. It can be applied to improve the resolution of microdevices such as bio-sensors and organic electronics.[22,23] Since the selective nanostructuring with a period of several micrometers, as shown in Figs. 2 and 3, is required to realize the unconventional petal surface, the HIL technique could be one of the most promising and practical solutions for bio-inspired engineering.

In addition, another promising application could be the fabrication of hybrid optics. Conventionally, nanostructures with a periodicity less than a wavelength have been applied

for diffractive optics. Otherwise, the periodical microstructures with a period longer than a wavelength have been used to uniformly diffuse the optical energy. Since the micro/nanoscale hybrid structured surface can coincidently represent both diffraction and diffusion in the same domain, these distinct optical properties can be integrated into a single device by using the HIL technique. In addition, optimizing HIL may enable the fabrication of high-efficiency and low-cost waveguides based on photonic crystal defects.[24]

This study was supported by National Research Foundation of Korea (NRFK) grant funded by the Korean government (Ministry of Education, Science and Technology) (Grant No. 2012-010307) and Gyeongnam National University of Science and Technology Grant. We thank Dr. Christopher Evans for his precious consultations.

[1]R. C. Jaeger, *"Lithography". Introduction to Microelectronic Fabrication*, 2nd ed. (Prentice Hall, Upper Saddle River, 2002).
[2]S. Ahn, K. Lee, J. Kim, S. H. Kim, S. H. Lee, J. Park, and P. Yoon, Microelectron. Eng. **78–79**, 314 (2005).
[3]M. L. Schattenburg, C. R. Canizares, D. Dewey, K. A. Flanagan, M. A. Hamnett, A. M. Levine, K. S. K. Lum, R. Manikkalingam, T. H. Markert, and H. I. Smith, Opt. Eng. **30**, 1590 (1991).
[4]M. Campbell, D. N. Sharp, M. T. Harrison, R. G. Denning, and A. J. Turberfield, Nature **404**, 53 (2000).
[5]C. O. Bozler, C. T. Harris, S. Rabe, D. D. Rathman, M. A. Hollis, and H. I. Smith, J. Vac. Sci. Technol. B **12**, 629 (1994).
[6]I. Byun and J. Kim, J. Micromech. Microeng. **20**, 055024 (2010).
[7]M. Mützel, S. Tandler, D. Haubrich, D. Meschede, K. Peithmann, M. Flaspöhler, and K. Buse, Phys. Rev. Lett. **88**, 083601 (2002).
[8]T. A. Savas, M. L. Schattenburg, J. M. Carter, and H. I. Smith, J. Vac. Sci. Technol. B **14**, 4167 (1996).
[9]C. Chang, Y. Zhao, R. K. Heilmann, and M. L. Schattenburg, Opt. Lett. **33**, 1572 (2008).
[10]S. Ahn, K. Lee, J. Kim, S. Kim, J. Park, S. Lee, and P. Yoon, Nanotechnology **16**, 1874 (2005).
[11]Z. Yu, W. Wu, L. Chen, and S. Y. Chou, J. Vac. Sci. Technol. B **19**, 2816 (2001).
[12]L. D. Sio, S. Serak, N. Tabiryan, S. Ferjani, A. Veltri, and C. Umeton, Adv. Mater. **22**, 2316 (2010).
[13]H. J. Tiziani, Proc. SPIE **1553**, 490 (1991).
[14]L. McMackin, D. G. Voelz, and M. P. Fetrow, Opt. Express **1**, 332 (1997).
[15]W. H. Steel, *Interferometry* (Cambridge University Press, Cambridge, 1986).
[16]W. B. Bridges and A. N. Chester, Appl. Opt. **4**, 573 (1965).
[17]D. Wang, Z. Wang, Z. Zhang, Y. Yue, D. Li, and C. Maple, Appl. Phys. Lett. **102**, 081903 (2013).
[18]T. B. O'Reillya and H. I. Smith, J. Vac. Sci. Technol. B **26**, 128 (2008).
[19]See supplementary material at http://dx.doi.org/10.1063/1.4841435 for PR structure in interstate HIF region.
[20]L. Feng, S. Li, Y. Li, H. Li, L. Zhang, J. Zhai, Y. Song, B. Liu, L. Jiang, and D. Zhu, Adv. Mater. **14**, 1857 (2002).
[21]L. Feng, Y. Zhang, J. Xi, Y. Zhu, N. Wang, F. Xia, and L. Jiang, Langmuir **24**, 4114 (2008).
[22]J. Kim, H. Park, B. Kang, R. Ku, C. Ham, and M. Yang, J. Appl. Phys. **110**, 084701 (2011).
[23]B. Kang, J. Kim, and M. Yang, Opt. Express **20**, 29111 (2012).
[24]P. V. Braun, S. A. Pruzinsky, and F. Garcia-Santamaria, Adv. Mater. **18**, 2665 (2006).